The Use of Aqueous Alkaline Hydrolysis to Reveal the Fine Structure of Poly(ethylene Terephthalate) Fibers

MARTHA J. COLLINS,* S. HAIG ZERONIAN,† and MARY SEMMELMEYER‡

Division of Textiles and Clothing, University of California, Davis, Davis, California 95616

SYNOPSIS

The fine structure and physical properties of bright and semidull poly(ethylene terephthalate) (PET) fibers were investigated as successive layers of the polymer were removed by hydrolysis using aqueous solutions of sodium hydroxide up to weight losses of 90 and 68%, respectively. For both types large changes in molecular weight distribution did not occur, although as weight loss increased, the density of the remaining fiber increased. Alterations in fine structure with weight loss were also observed by thermal analysis. Greater strength loss with decreasing weight occurred for the semidull fiber than for the bright sample. Larger pits formed on the surface of the hydrolyzed semidull fibers than on the surface of the bright products. This observation is attributed to the titanium oxide present in the semidull fibers. It was also noted that as the density of the bright PET samples was increased by heatsetting, the rate of hydrolysis decreased.

INTRODUCTION

Recently, we published a critical review of research on the reaction between poly(ethylene terephthalate) (PET) fibers and bases.[1a] From the evidence presented in that article it can be concluded that aqueous sodium hydroxide reacts in a topochemical manner with PET. Thus, as the reaction proceeds, surface layers are successively removed by hydrolysis. In contrast, low molecular weight amines will react in a permeant manner with PET fibers and thus degradation will take place throughout the sample. Aminolysis has been used as a technique for studying fiber[1a] and film[1b] structure by selective etching. However, aminolysis destroys the integrity of the fiber. The question then is whether some aspects of fiber structure could be better studied by hydrolysis with aqueous alkali metal hydroxides.

Thus, the objective of this work was to further characterize alkali-hydrolyzed PET. An additional objective was to determine if aqueous alkaline hydrolysis could be used to evaluate whether any differences occurred in the properties of the PET fiber as successive layers were removed. To this end, bright and semidull PET samples were obtained and the physical properties of nonhydrolyzed, or control, and hydrolyzed samples were characterized.

EXPERIMENTAL

Materials

The starting materials were heatset delustered (approximately 0.2% TiO_2 by weight) Dacron PET type 56T fabric (obtained from Test Fabrics, Inc., Middlesex, NJ) made of multifilament yarns and an experimental bright (0% TiO_2) PET multifilament yarn supplied by Du Pont de Nemours Co., Inc. All chemicals used were reagent grade.

Methods of Treatment

Alkaline Hydrolysis

Semidull samples were treated in 2.8*M* NaOH, 1% cetyltrimethylammonium bromide (CTAB) (w/w) solution at 60°C (±0.1°C) by a procedure described

* Current address: Union Carbide Corporation, Technical Center Research and Development, P.O. Box 8361, S. Charleston, WV 25301.

† To whom correspondence should be addressed.

‡ Current address: Clorox Technical Center, Pleasanton, CA 94566.

Journal of Applied Polymer Science, Vol. 42, 2149–2162 (1991)
 CCC 0021-8995/91/082149-14$04.00

elsewhere.[2] Bright yarns were treated in 2.5*M* NaOH, 0.1% CTAB solution in sealed jars at 21°C (±2°C) with mild mechanical agitation. All samples were treated in a 2.5 ratio of weight/volume (g/L). In both cases, CTAB was added to accelerate the hydrolysis. Pretesting had determined that CTAB had no effect on the characterized physical properties of the PET products.

To terminate the hydrolysis, samples were rinsed in deionized water to remove excess NaOH and neutralized for 2 min in 0.1% HCl. The specimens were then washed in deionized water until the rinse water was neutral to litmus paper. The products were blotted and spread on filter paper and allowed to air dry to constant weight in a constant temperature and humidity (CTH) room at 21°C and 65% relative humidity. For each series of samples prepared, a semidull control was treated for 2 h and a bright control was treated for 72 h in the exact manner as the hydrolyzed specimens using solutions without sodium hydroxide.

Heatsetting Bright Yarns

For each of the heatsetting temperatures (125, 150, 175, and 197°C), four replicate hanks were prepared. Approximately 0.5 g samples were prepared by wrapping the yarn onto a metal rectangular specimen holder under 0.8 g tension. The yarn ends were tied off and the specimen holder, containing all four samples, was placed in a horizontal position in a preheated oven. After 30 min, the samples were removed from the oven and allowed to cool for 24 h before the products were removed from the device. The areas where the yarns had been in contact with the metal holder were marked to ensure they were not used for any physical testing.

Characterization of Products

Weight Loss

The weight loss of the semidull samples was determined from the difference in tex (i.e., weight in g of 1000 m of filament) of warp yarn which had been unravelled from the control and hydrolyzed fabric samples and then conditioned in the CTH room. The weight loss for the bright samples was determined by weighing the conditioned specimens before and after hydrolysis.

Tex

Tex was measured for the control and hydrolyzed semidull warp yarns and the control bright yarn in the standard manner.[3] The bright multifilament yarns did not maintain their yarn integrity after hydrolysis; therefore, their tex was calculated using the weight loss of the treated yarns and the tex value of the control yarn. Fiber tex was obtained by dividing the yarn value by the number of fibers in the starting yarn.

Fiber Radius

Fiber radius was determined by measuring the diameter of fibers mounted in glycerol on microscope slides using a Cambridge Quantimet 900 image analyzer. The value for a sample was calculated by taking 39 measurements on each of 25 fibers.

Gel Permeation Chromatography (GPC)

Molecular weight distributions were determined using a Perkin-Elmer (PE) liquid chromatography Series 10 unit fitted with two Water's Ultrastyragel GPC columns (sizes 1000 and 50 nm) and 70/30 dichloromethane/hexafluoroisopropanol as the solvent and mobile phase[4] using a UV detector at 254 nm. Data were collected and analyzed with the aid of PE CHROM2 software.

The system was calibrated using a plot of $\log(M_w)$ versus retention time fitted by third-order polynomial regression using four PET fractions of varying intrinsic viscosity, prepared from broad polymer using preparative GPC, and the PET cyclic trimer.[5] The calibration curve was checked with a broad PET standard. The differential molecular weight distribution curves were determined[6] using the digitized heights up to but not including the trimer peak. The validity of trimer exclusion was verified.[5] Chromatograms were determined in at least duplicate.

Density

Determinations were made with a density gradient column prepared with mixed xylenes and perchloroethylene and maintained at a temperature of 21°C (±2°C). Results are the average of at least four replicates.

Differential Thermal Analysis (DTA)

Duplicate measurements were made with a Mettler TA 2000M thermal analysis system in a nitrogen atmosphere at a heating rate of 5°C/min using approximately 4.5 mg samples. Temperatures were read directly from the DTA scans and heats of fusion were obtained from the area of the melting endotherm.[7]

Table I Physical Characteristics of Bright and Semidull PET Fibers

Hydrolysis Time (h)	Weight Loss (%)	Filament Decitex	Radius (μm)[a]	Bulk Density (g/cm^3)	Radial Density (g/cm^3)[b]
		Semidull Fibers			
Control	0.0	5.1	11.1 (.2)	1.389	1.387
0.5	3.5	5.0	10.7 (.1)	1.389	
1.0	13.7	4.4	10.3 (.0)	1.390	
2.0	28.5	3.7	9.4 (.0)	1.390	
3.0	39.0	3.1	8.9 (.1)	1.390	
4.0	48.8	2.6	8.1 (.1)	1.391	1.391
5.0	61.5	2.0	6.8 (.0)	1.390	
6.0	68.3	1.6	6.5 (.1)	1.391	
		Bright Fibers			
Control	0.0	3.3	9.1 (.1)	1.370	1.367
2.0	3.1	3.2	8.8 (.1)	1.370	
4.0	5.6	3.1	8.7 (.1)	1.371	
8.8	16.7	2.7	8.2 (.1)	1.371	
22.2	40.5	2.0	7.0 (.1)	1.372	1.369
50.0	69.1	1.0	4.9 (.1)	1.375	1.372
52.2	73.9	0.9	—	1.374	
69.1	90.9	0.3	2.9 (.1)	1.381	1.381

[a] Standard error in parentheses.
[b] Calculated from eq. (1).

Scanning Electron Microscopy (SEM)

Scanning electron micrographs were obtained in the manner described previously.[8]

Fiber Tensile Properties

Measurements were made on a table model Instron universal testing machine with a 2.54 cm gauge length at 2 cm/min constant rate of elongation at 65% relative humidity and 21°C. Results are an average of 25 tests.

RESULTS AND DISCUSSION

Weight Loss

Both the semidull samples and the bright samples follow the established linear relationship for weight loss vs. treatment time for aqueous alkaline hydrolysis of PET (Table I) with correlation coefficients of 0.995 and 0.994 for the two plots (Fig. 1), respectively.[9] The semidull PET was treated at 60°C, whereas the bright PET was treated at only 21°C, since it hydrolyzed rapidly at 60°C (during pretesting, hydrolysis at 60°C destroyed the structure of the bright filaments before 6 h). The greater reactivity of the bright sample is attributed mainly to such factors as the following: First, it had greater surface area per unit weight; about 20% more than the semidull sample. Second, the density of the bright samples was lower (Table I). Third, there would have been increased access of the reagent to the filament surfaces in the loose bright yarns than to those in the semidull fabric. As will be discussed later, when the density of the bright yarn was increased by heatsetting, its reactivity to hydrolysis

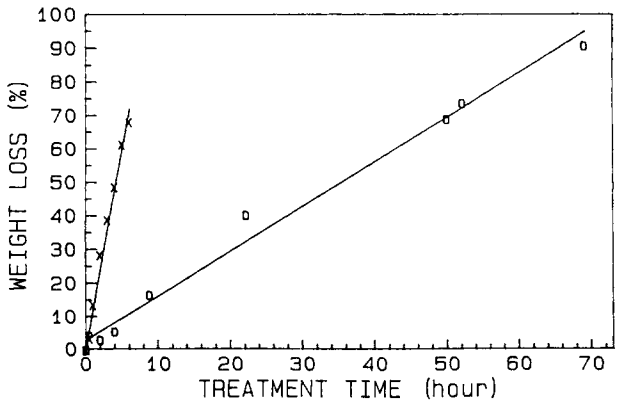

Figure 1 Weight loss vs. treatment time for bright and semidull samples: (×) semidull; (○) bright.

Table II Density and Weight Loss of Bright Yarns Heatset at Constant Length at Different Temperatures and Then Hydrolyzed

Hydrolysis Time (h)	Heatset Temperature (°C)	Weight Loss (%)	Density (g/cm^3)
0	—	0.0	1.370
0	125	0.0	1.374
0	150	0.0	1.379
0	175	0.0	1.386
0	197	0.0	1.388
72	—	79.5	1.376
72	125	61.6	1.377
72	150	45.8	1.381
72	175	36.2	1.388
72	197	20.8	1.389
96	125	68.3	1.376
96	150	50.2	1.380
96	175	40.6	1.388
96	197	32.3	1.389

decreased markedly (Table II). It is stressed that the heatset bright samples were also hydrolyzed at 21°C so that their reactivity can be compared to that of the nonheatset sample.

Equations have been derived relating the initial radius of cylindrical fibers and the square root of the percent residual weight of the sample at any given time utilizing the aqueous hydrolysis rate constant.[10] However, since the rate constant for hydrolysis is dependent on a variety of factors, including temperature, solution molarity, and starting sample physical characteristics,[1a] the rate constant must be determined for each set of conditions.

A relationship can also be derived for cylindrical fibers to predict final radius based on only initial radius and percentage weight loss. If it is assumed that length and density remain constant, the equation for final radius of a cylindrical fiber at any weight loss is

$$r_f = [r_i^2(1 - \mathrm{FWL})]^{0.5} \qquad (1)$$

where r_f is the final radius and r_i is the initial radius and FWL is the fractional weight loss.

As seen in Table III, the measured and calculated values of radii for both semidull and bright fibers using eq. (1) are very close. The fact that the fibers retain their cross-sectional geometry with weight loss has been used as empirical evidence pointing to the surface characteristic of this reaction.[9,10]

Linear regression of a plot of measured radius versus time yields lines with correlation coefficients of 0.995 and 0.997 for both semidull and bright fibers, respectively (Fig. 2). If this linear relationship is extrapolated to zero radius, it would take 14 h at 60°C to fully hydrolyze the semidull and 105 h at 21°C to hydrolyze the bright samples.

The predictability of fiber radius up to a weight loss of 68 and 91% is remarkable (Table III). Based on the solid cylindrical model, as hydrolysis progresses, surface area per unit weight increases. Yet, with increasing hydrolysis, the absolute weight of the specimen is lessening; therefore, the absolute surface area available during the experiment is really decreasing. In fact, however, due to pitting taking place as hydrolysis occurs,[1] the true surface area will be greater than the geometric surface area.[11] It appears that the weight loss that occurs is being counterbalanced by the increase in surface area of the sample. Fiber pitting is discussed in a later section of this paper.

A small increase in sample density occurred on heatsetting (Table II), indicating an increase in

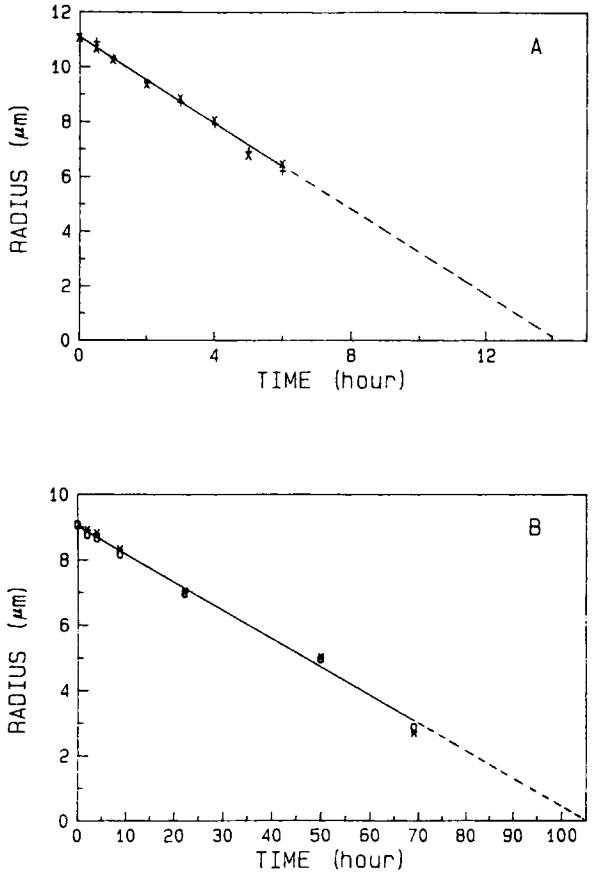

Figure 2 Predictions of radius using weight loss vs. time and measured radius vs. time. (A) semidull: (×) measured; (+) calculated. (B) Bright: (○) measured; (∗) calculated.

Table III Radius Predictions for Hydrolyzed PET Fibers

Hydrolysis Time (h)	WL[a] (%)	Measured Radius (μm)	Calculated Radius[b] (μm)	Predicted Radius from Measured Radius vs. Time[c] (μm)
		Semidull		
0.0	0.0	11.1	—	11.1
0.5	3.5	10.7	10.9	10.7
1.0	13.7	10.3	10.3	10.3
2.0	28.5	9.4	9.4	9.5
3.0	39.0	8.9	8.7	8.7
4.0	48.8	8.1	7.9	7.9
5.0	61.5	6.8	6.9	7.2
6.0	68.3	6.5	6.2	6.4
7.0	—	—	—	5.6
8.0	—	—	—	4.8
8.2	—	—	—	4.6
8.4	—	—	—	4.5
10.0	—	—	—	3.2
11.0	—	—	—	2.4
12.0	—	—	—	1.6
13.0	—	—	—	0.8
14.0	—	—	—	0.0
		Bright		
0.0	0.0	9.1	—	9.0
2.0	3.1	8.8	8.9	8.9
4.0	5.6	8.7	8.8	8.9
8.8	16.7	8.2	8.3	8.3
22.2	40.5	7.0	7.0	7.1
50.0	69.1	5.0	5.0	4.7
69.1	90.9	2.9	2.7	3.1
72.5	—	—	—	2.8
73.1	—	—	—	2.7
80.0	—	—	—	2.1
90.0	—	—	—	1.3
100.0	—	—	—	0.4
104.7	—	—	—	0.0

[a] Weight loss.
[b] From eq. (1).
[c] Radius = $11.1 - 0.789t$, $r = 0.995$ for semidull; radius = $9.02 - 0.086t$, $r = 0.998$ for bright.

crystallinity. The samples had been heatset in constant length positions to prevent shrinkage so that the diameters of the fibers would be similar and a relative comparison of the hydrolysis rates could be made. In fact, the diameters of the starting fiber (9.1 μm) and the heatset fibers (8.6, 8.9, 8.8, and 8.8 μm for the 125, 150, 175, and 197°C heatset temperatures, respectively) were not markedly different.

Since alkaline hydrolysis appears to take place at fiber surfaces, it may be thought that fine structure would not influence the rate at which hydrolysis occurs. However, it was observed that, as the density of bright yarns was increased by heatsetting, the rate of weight loss decreased (Table II). Because the density of a semicrystalline material consists of a summation of the density of the crystallite units (of various sizes and degrees of perfection) and the lesser ordered regions, it appears that the rate of hydrolysis is affected by any changes of molecular order and of the molecular forces between PET chains at the reaction interface. It is suggested that preferential penetration and reaction occurs in nonordered regions present at the surface of the filaments and that a decrease occurs in the amount of

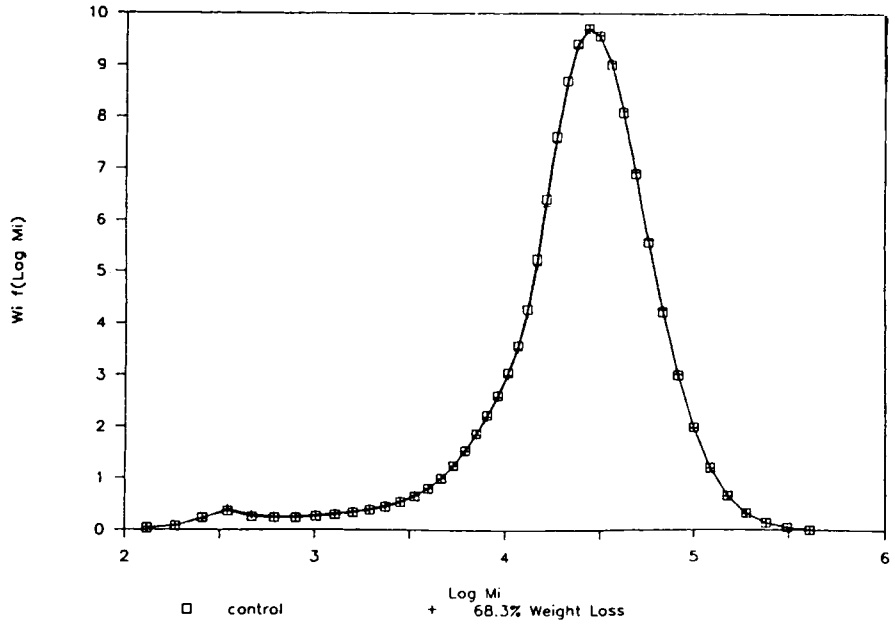

Figure 3 Differential molecular weight distributions for nonhydrolyzed semidull polyester and its counterpart after 68.3% weight loss.

wetting or swelling at the solid–solution interface as interchain cohesiveness is increased by heatsetting.

Molecular Weight Distributions

The viscosity average molecular weights,[12,13] intrinsic viscosities,[2,8,14] and number average molecular weights[12] have been determined for caustic hydrolyzed PET. However, the complete molecular weight distributions of hydrolyzed fibers gives a superior representation of any fine changes in the molecular weight of the polymer. The differential molecular weight distribution (DMWD) of the nonhydrolyzed semidull PET (Fig. 3) was typical of distributions obtained by others for a commercial PET of this

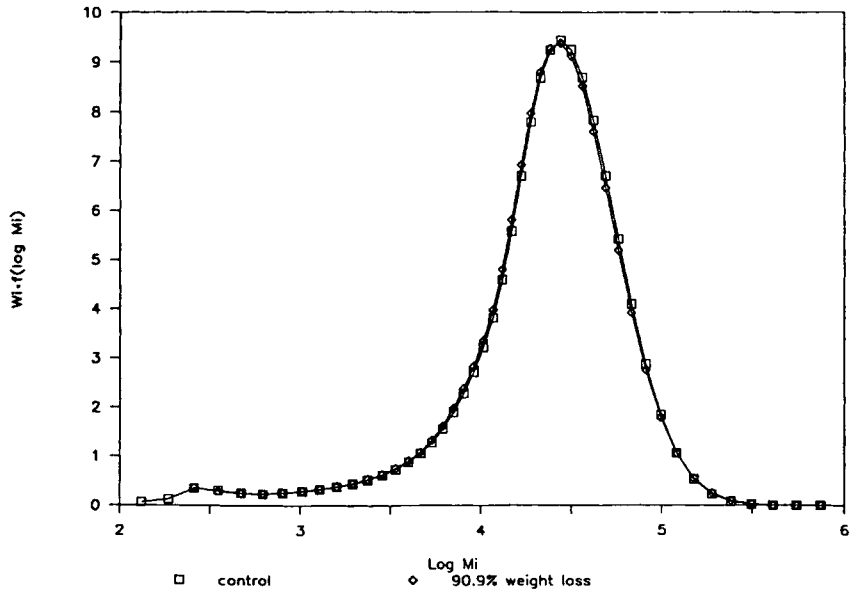

Figure 4 Differential molecular weight distributions for nonhydrolyzed bright polyester and its counterpart after 90.9% weight loss.

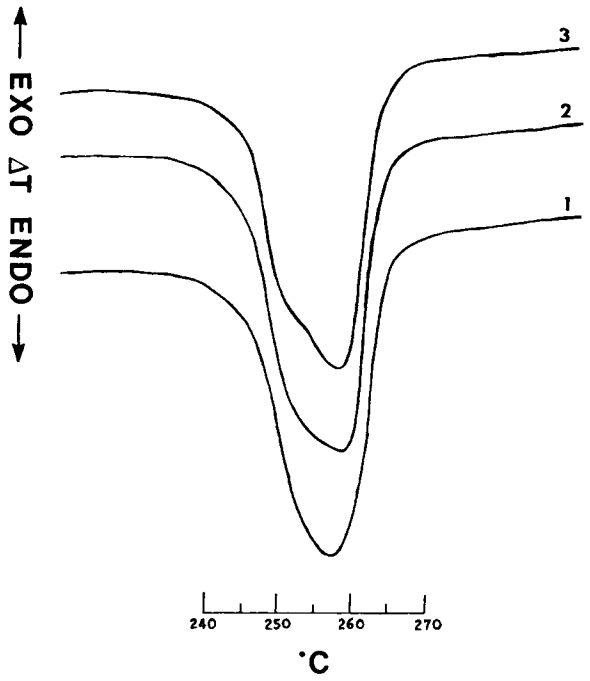

Figure 5 Melting endotherms of bright polyester: (1) starting; (2) heatset at 150°C; (3) heatset at 197°C.

type.[4,15] Only small changes in the DMWD were observed after hydrolysis. For example, the DMWD of the semidull sample which had suffered 68.3% weight loss was identical to its control. Also, there was no change in the DMWD for the 197°C heatset bright sample of 20.8% weight loss. However, for the nonheatset bright sample of 90.9% weight loss, there was a small increase in the lower molecular weight components (Fig. 4), although no change in the peak average molecular weight was observed.

Most researchers have found no evidence of large molecular weight changes with alkaline hydrolysis, although one worker has reported a substantial increase in end groups[16] with hydrolysis of PET to weight losses of only 8%. If there had been a large increase in number average molecular weight, then a marked shift in the DMWD would have been observed; much larger than the small shoulder actually seen on the 90.9% weight loss sample. The change in DMWD by 90.9% weight loss may be due to deposit of hydrolyzed products at the fiber surface, which would become apparent in the DMWD when the polymer molecules at the surface become a large enough portion of the bulk to be significant.

Generally, it can be concluded from this data that there are no major changes in the DMWD as the

Table IV Enthalpy (ΔH_f) and Temperatures of Shoulder (T_{m1}) and Zenith (T_{m2}) of the Melting Endotherm of PET Samples

Sample Treatment	Weight Loss (%)	T_{m1} (°C)	T_{m2} (°C)	ΔH_f (kJ/kg)
	Semidull Fibers			
None	—	—	261.6	49.9
HDZ[a]	68.3	—	261.6	52.5
	Bright Fibers			
None	—	—	257.2	50.5
HDZ[a]	40.5	—	257.3	50.6
HDZ	69.1	—	257.1	51.5
Heatset 150°C	—	251	259.1	51.4
Heatset and HDZ	45.8	—	257.2	49.6
Heatset 197°C	—	251	258.6	50.1
Heatset and HDZ	20.8	251	257.4	50.5

[a] HDZ = hydrolyzed with aqueous NaOH.

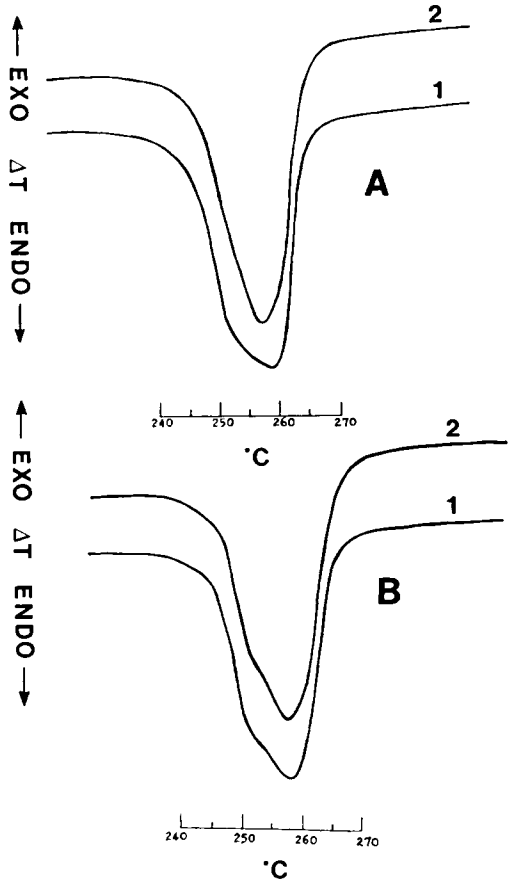

Figure 6 Melting endotherms of bright samples before and after various treatments. A: (1) Heatset 150°C control; (2) after 45.8% weight loss. B: (1) Heatset 197°C control; (2) after 20.8% weight loss.

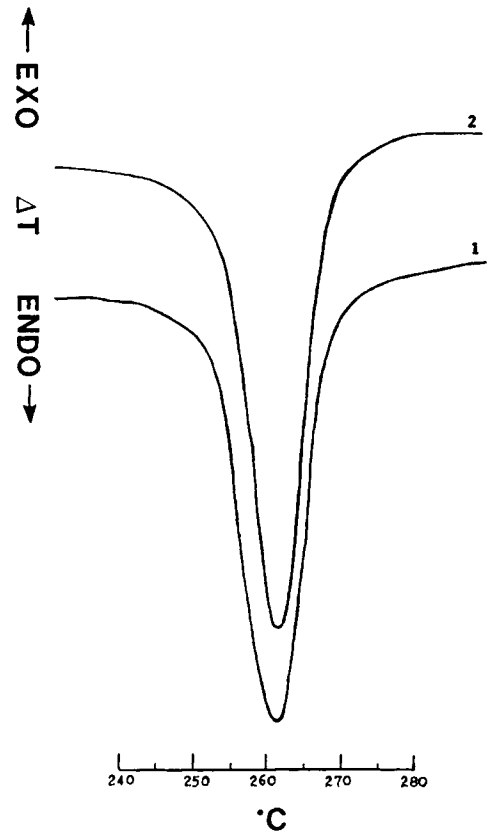

Figure 7 Melting endotherms for semidull samples: (1) control; (2) after 68.3% weight loss.

center of the fibers is approached and thus the bright and semidull fibers are homogeneous with respect to this property.

Density

For all samples, the density of the hydrolyzed fibers increased with increasing time of hydrolysis (Tables I and II). In the case of the semidull samples, the increase is considered significant only in the context of the changes observed in the density of the bright and heatset bright samples.

An equation can be derived for the density of successive layers in the PET fibers by considering mass, volume, and density as additive functions and assuming that fiber length does not change during hydrolysis. Then

$$m_t = m_1 + m_c \tag{2}$$

where m_t, m_1, and m_c are the masses of the starting product, the removed layer, and the remaining core, respectively. Dividing eq. (2) by the volume of the starting product (v_t), we obtain

$$\rho_t = (m_1 + m_c)/v_t \tag{3}$$

where ρ_t is the density of the starting sample. Equation (3) can be transformed by expressing the total volume in terms of the volume fractions of the removed layer (Θ_1) and the remaining core (Θ_c):

$$\Theta_1 = v_1/v_t = \pi l(r_t^2 - r_c^2)/\pi r_t^2 l \tag{4}$$

$$\Theta_c = v_c/v_t = \pi r_c^2 l/\pi r_t^2 l \tag{5}$$

where l is the fiber length and

$$\rho_t = \rho_1\Theta_1 + \rho_c\Theta_c \tag{6}$$

where ρ_1 and ρ_c are the densities of the removed layer and remaining core, respectively, or,

$$\rho_t = \rho_1(1 - r_c^2/r_t^2) + \rho_c(r_c^2/r_t^2) \tag{7}$$

Densities of radial layers as the hydrolysis progresses are calculated (Table I) using eq. (7) at levels of significant density changes in each sample.

It will be observed from the calculated radial densities that the outer portions of the fibers are significantly less dense than the core. It appears, therefore, that the semicrystalline structure of the fibers is not a homogeneous arrangement. This does not seem implausible; such factors as the differential shear force on the polymer molecules flowing through a spinneret, the drawing process, and a heat differential during cooling due to the heat capacity of the substance could all influence the differences in molecular arrangement depending on location in the fiber structure.

Thermal Properties

Comparison of the melting endotherms of the bright control and heatset samples (Fig. 5) illustrates the changes in the crystalline fine structure of this product as heatset temperature increases. The sample heatset at 150°C developed a shoulder on the low temperature side of the peak and the temperature of the zenith of the melting region was distinctly higher (Table IV). The sample treated at 197°C resembled the 150°C sample, but the shoulder appeared more defined and the temperature of the zenith was slightly lower.

A double peak melting endotherm for PET fibers has been reported[17] and the regions in the double peak PET endotherm have been defined as types I

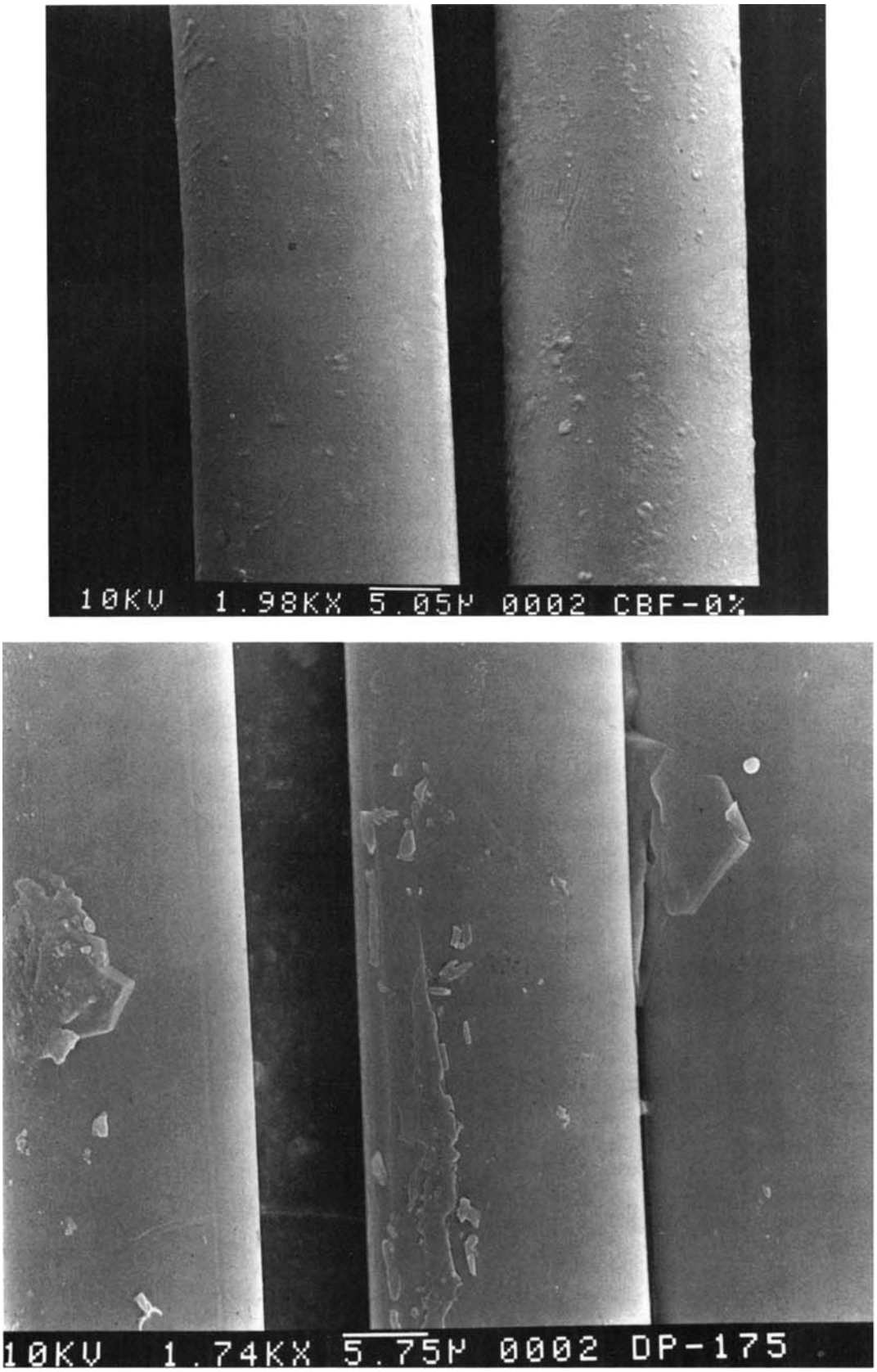

Figure 8 Scanning electron micrographs of control and heatset bright fibers: (A) control; (B) heatset at 197°C.

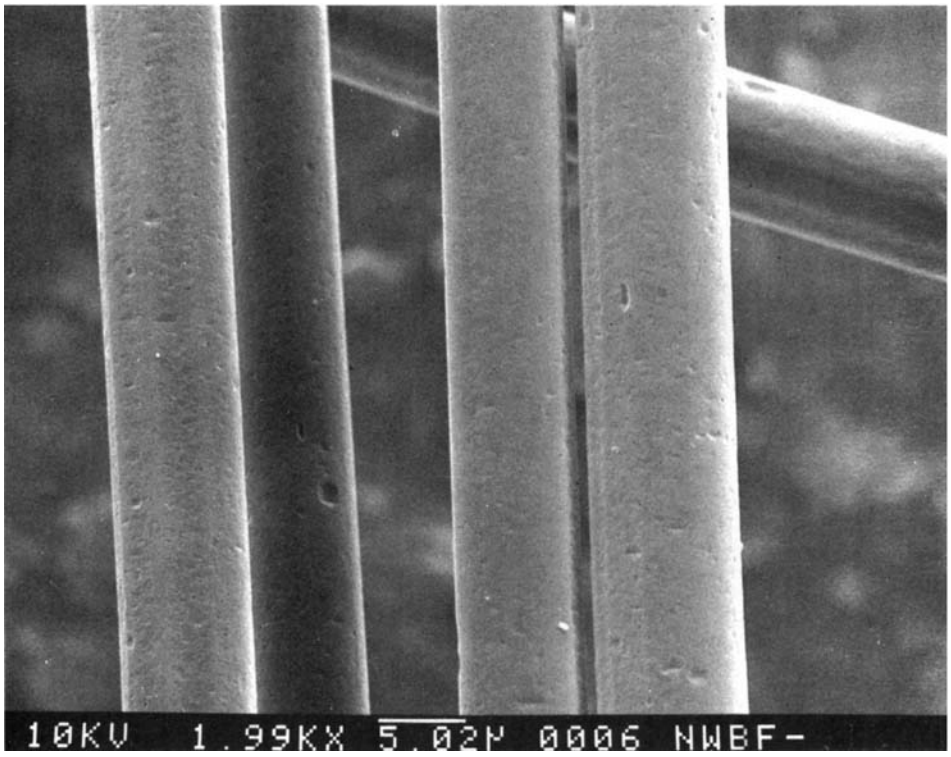

Figure 9 Scanning electron micrographs of hydrolyzed bright fibers, 79.5% weight loss.

and II. Type I, or stable fraction, melts at a lower temperature than type II, or less stable fraction, which undergoes reorganization during the DTA run. Thus, the constant length heatsetting of the bright PET sample may have induced some separation into these two crystallite types, where type I is seen as a shoulder on the endotherm (Table IV).

When the bright samples were hydrolyzed to 40.5 and 69.1% weight loss, the endotherms and the heats of fusion were essentially the same (Table IV). With 150°C heatsetting, [Fig. 6(a)] the low temperature shoulder disappeared with a 45.8% weight loss obtained by hydrolysis and the zenith of the melting region shifted to a lower temperature. The sample heatset at 197°C had no change in the heat of fusion by 20.8% weight loss [Fig. 6(b)] but had a sharpening of the endotherm along with a decrease in the melting point. These phenomena may indicate that the lower melting crystallites are located in the exterior portion of the bright fibers with the higher melting species present in the inner regions.

The peak melting temperature of the control and hydrolyzed semidull fibers (Fig. 7), which was heatset commercially, were similar. However, the melting endotherm appeared to become sharper and the enthalpy became larger on hydrolysis.

Scanning Electron Microscopy

The starting bright fibers [Fig. 8(a)] were relatively smooth and cylindrical. On heatsetting at 150°C and 197°C, they exhibited surface oligomer deposits characteristic of migration to the surface during constant-length heatsetting [Fig. 8(b)].[18] After hydrolysis, both the starting and heatset bright fibers formed small circular-shaped pits on their surfaces. The pits increased in size somewhat as high weight losses were achieved. This phenomenon is illustrated in Figure 9 for a sample which had suffered extensive weight loss. No signs of oligomers remained on the surfaces of heatset bright fibers after hydrolysis. In contrast, when titanium dioxide (TiO_2) was present in the fiber matrix, as hydrolysis progressed deep cavities formed which ran parallel to the fiber axis [Fig. 10(a) and 10(b)]. Particles were observed to be dispersed fairly uniformly on the fiber surface and, in some cases, in the pits themselves. It has been shown[19] that in PET fibers that the areas where high concentrations of TiO_2 are found are void-containing areas. When PET fibers were strongly etched in a glow discharge with argon, the TiO_2 particles were observed to stand out from voids which were elliptical in shape and ran parallel to the fiber axis.[19]

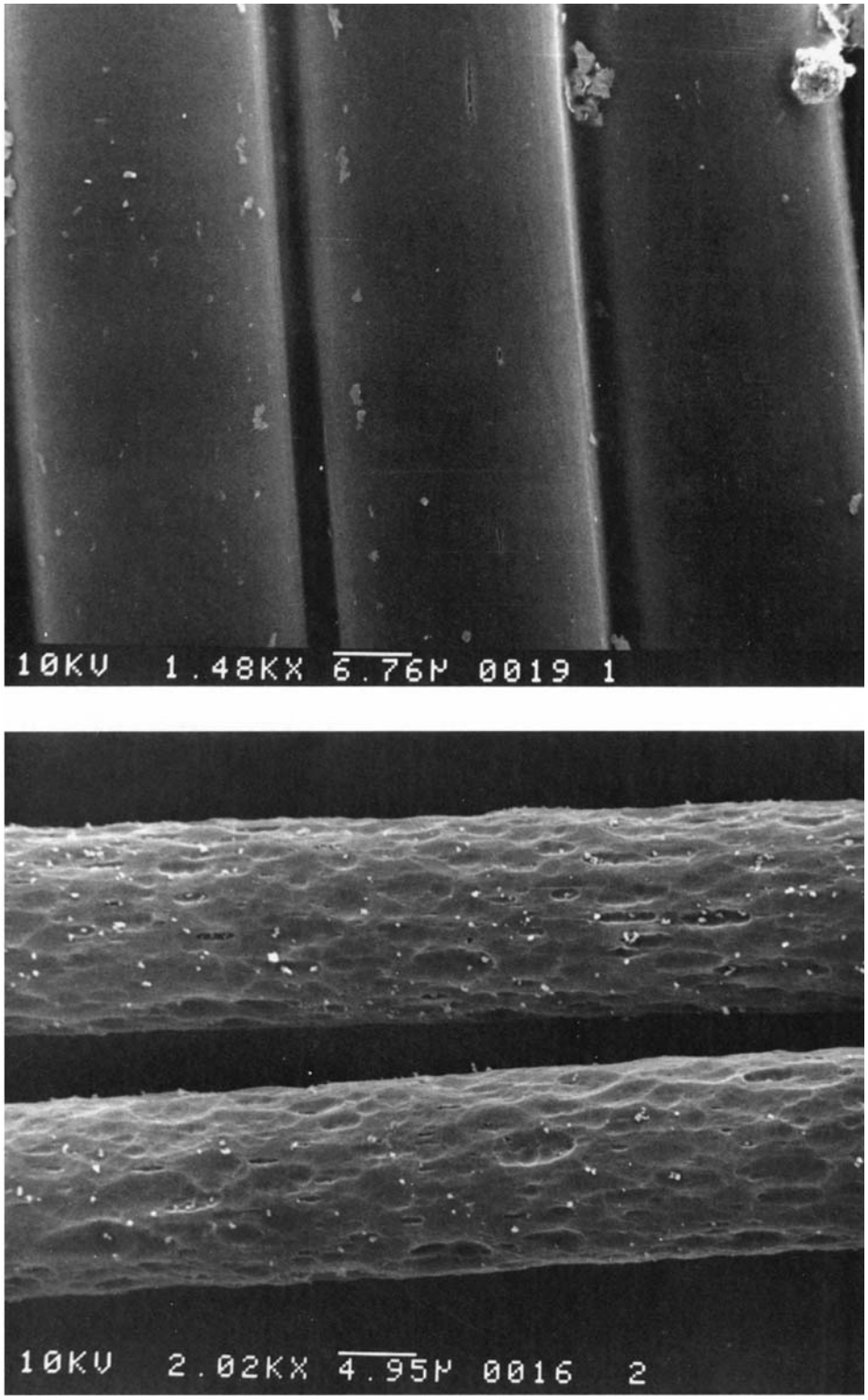

Figure 10 Scanning electron micrographs of control and hydrolyzed semidull fibers: (A) control; (B) 68.3% weight loss.

Table V Changes in Tensile Properties of Fibers on Hydrolysis

Weight Loss (%)	Ultimate[a] Stress (kJ/kg)	Breaking[a] Strain (%)	Initial[a] Modulus (kJ/kg)
		Semidull	
0.0	410 (5)	34.7 (1.1)	2820 (76)
3.5	384 (3)	30.0 (0.6)	2690 (59)
13.7	383 (6)	28.3 (1.2)	3140 (133)
28.5	360 (5)	24.0 (0.9)	3100 (80)
39.0	345 (6)	22.3 (0.8)	2890 (93)
48.8	332 (8)	20.1 (0.9)	3310 (74)
61.5	281 (4)	17.8 (0.6)	3200 (90)
68.3	237 (8)	11.0 (0.5)	3310 (60)
		Bright	
0.0	374 (8)	42.6 (1.6)	4010 (111)
3.1	356 (9)	39.1 (1.7)	4770 (108)
5.6	355 (5)	34.2 (1.1)	4890 (88)
16.7	357 (5)	35.5 (1.2)	5170 (122)
40.5	333 (6)	36.8 (0.7)	4150 (117)
69.1	283 (10)	20.1 (1.4)	4600 (160)
79.5	232 (10)	12.0 (0.9)	5860 (413)
90.9	203 (20)	8.7 (0.8)	3550 (241)

[a] Standard error in parentheses.

Solbrig and Obendorf [20] suggested that the large cavities, due to alkaline hydrolysis are amorphous regions, and reported that TiO_2 particles were found in the vicinity of the severely pitted regions.

If the areas in the fibers where TiO_2 appear to be located can be considered defects in terms of being either less ordered (amorphous) or void regions, then the pits which are formed and appear to enlarge as hydrolysis progresses can be interpreted as evidence of structural imperfections. The fact that

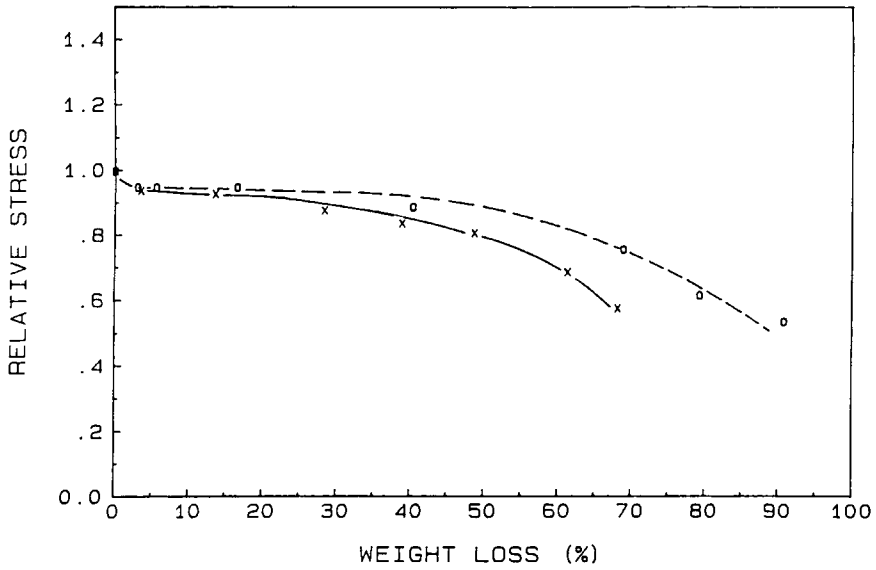

Figure 11 Relative ultimate stress versus weight loss (%) for bright and semidull hydrolyzed fibers: (×) semidull; (○) bright.

roughening and circular-shaped pits were observed on all of the hydrolyzed bright fiber products could be indicative of the presence of inorganic impurities in these samples.

Tensile Properties

A loss in ultimate stress occurred for both the semidull and the bright fibers as weight loss increased (Table V and Fig. 11). The range of weight loss characteristic for commercial hydrolyses is usually not greater than 30%.[1a] In earlier studies a straight line with a slope close to zero has been drawn through the origin for the plot of tenacity versus weight loss or a slope close to 1 for strength versus weight loss at these lower weight losses.[13,21] However, it is now apparent that a small loss in specific stress does occur initially before specific stress becomes approximately constant with increasing weight loss. Finally at weight losses of higher than about 30% the rate of decrease of specific stress with increasing weight loss accelerates.

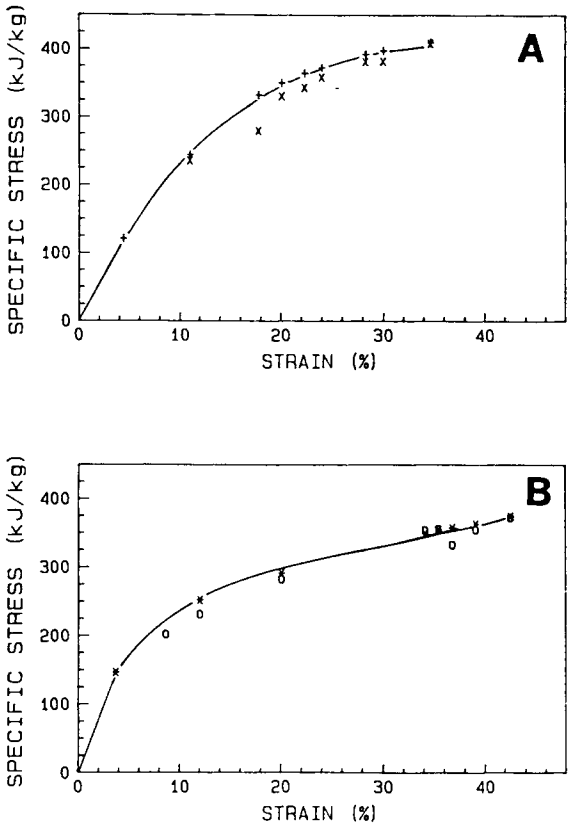

Figure 12 Ultimate stress versus strain for bright and semidull fibers. (A) Semidull: (+) stress/strain curve for control; (×) ultimate stress/strain for hydrolyzed. (B) Bright: (*) stress/strain curve for control; (○) ultimate stress/strain for hydrolyzed.

Because the molecular weight distributions were essentially unaffected by hydrolysis, the morphological variations caused by the surface roughness and pits may be considered the primary cause of failure in the fibers by introducing weak points or defects at which rupture is initiated. This is especially apparent by the initial drop in relative stress for both samples with the onset of surface irregularities and pits. Using SEM, we observed pit formation beginning in the bright fiber hydrolyzed to only 3.1% weight loss. The weight loss region where specific stress remains roughly constant reflects no further change in failure mechanism. The final marked decrease in stress at higher weight losses illustrates the increasing influence of the surface morphology as the cross-sectional area of the fiber is reduced.

By plotting ultimate stress versus strain for the hydrolyzed fibers (Fig. 12) it will be observed that the changes in the hydrolyzed fibers' breaking stress and strain lie close to the specific stress/strain curve of the control PET. Thus no major changes in fiber structure have occurred. It will be noted also that the initial moduli of the fiber did not vary markedly with increasing weight loss (cf. Table V).

CONCLUSIONS

The evidence presented in this paper is consistent with the hypothesis that aqueous sodium hydroxide reacts topochemically with PET. It appears that aqueous alkaline hydrolysis can be successfully used to investigate differences in the structure of PET fibers since the reaction removes PET from the fiber periphery without degrading the residue.

REFERENCES

1. (a) S. H. Zeronian and M. J. Collins, *Text. Prog.*, **20**(2), 1 (1989). (b) W. P. Baker, *J. Appl. Polym. Sci.*, **57**, 993 (1962).
2. M. S. Ellison, L. D. Fisher, K. W. Alger, and S. H. Zeronian, *J. Appl. Polym. Sci.*, **27**, 247 (1982).
3. ASTM D1059-72, *Annual Book of ASTM Standards, Part 24, Textile Materials,* American Society of Testing and Materials, Philadelphia, 1972.
4. J. R. Overton and H. L. Browning, Jr., *ACS Symposium Series 245,* T. Provder, Ed., Am. Chem. Soc., Washington, DC, 1984, p. 219.
5. M. J. Collins, Ph.D. dissertation, University of California, Davis, 1989.
6. ASTM D3536-76, *Annual Book of ASTM Standards,*

Vol. 35, Part 8.02, Polymer Materials, American Society of Testing and Materials, Philadelphia, 1976.
7. *Mettler Instrument Manual: Differential Thermal Analysis.* Mettler Instrument Corp., Zurich, Switzerland, 1978, Chap. 7.
8. S. H. Zeronian, M. J. Collins, L. D. Fisher, and S. L. Hawk, *J. Ind. Fabrics,* **3,** 19 (1984).
9. E. Waters, *J. Soc. Dyers Colour.,* **66,** 609 (1950).
10. G. Valk and G. Stein, *Die alkalische hydrolyse physikalisch und chemisch modifizierter Polyesterfasern,* Forschungsbericht des Landes Nordrhein-Westfalen No. 2612, Westdeutscher Verlag, Opladen, 1977.
11. S. H. Zeronian, H.-Z. Wang, and K. W. Alger, *J. Appl. Polym. Sci.,* **41,** 527 (1990).
12. H. Hendrix, *Z. Ges. Textilind.,* **63,** 962 (1961).
13. J. Dave, R. Kumar, and H. C. Srivastava, *J. Appl. Polym. Sci.,* **33,** 455 (1987).
14. S. H. Zeronian and M. J. Collins, *Text. Chem. Color.,* **20**(4), 25 (1988).
15. K. Weisskopf, *J. Polym. Sci., Polym. Chem. Ed.,* **26,** 1919 (1988).
16. B. M. Latta, *Text. Res. J.,* **54,** 766 (1984).
17. V. B. Gupta, C. Ramesh, and A. K. Gupta, *J. Appl. Polym. Sci.,* **29,** 3728 (1984).
18. A. L. Cimecioglu, S. H. Zeronian, K. W. Alger, M. J. Collins, and G. C. East, *J. Appl. Polym. Sci.,* **32,** 4719 (1986).
19. J. W. S. Hearle and S. C. Simmens, *Polymer,* **14,** 273 (1973).
20. C. M. Solbrig and S. K. Obendorf, *Cell Abstract No. 10,* 192nd National Meeting, American Chemical Society, Anaheim, CA, September 1986.
21. S. M. Gawish and G. Ambroise. *Am. Dyestuff Rep.,* **75,** 30 (1986).

Received June 13, 1990
Accepted August 2, 1990